Advances in Nano Research, *Vol. 5, No. 2 (2017) 171-178*
DOI: https://doi.org/10.12989/anr.2017.5.2.171

Preparation of superparamagnetic $ZnFe_2O_4$ submicrospheres via a solvothermal method

Jie Ma *, Bingjie Chen [a], Bingkun Chen [b] and Shuping Zhang [c]

College of science, University of Shanghai for Science and Technology, Shanghai 200093, P.R. China

(*Received September 14, 2016, Revised November 26, 2016, Accepted April 08, 2017*)

Abstract. Superparamagnetic Zinc ferrite submicropheres are firstly synthesized via a one-pot solvothermal approach at 200-215°C for 4-8 hours. $ZnCl_2$, $FeCl_3$ and NaAc are used as precursors with ethylene glycol solvent. The X-ray diffraction (XRD) data indicate that $ZnFe_2O_4$ nanoparticles with the grain size around 15±3 nm can be successfully synthesized via the one-pot method. The scanning/transmission electronic microscope (SEM/TEM) images further show the samples are submicrospheres self-assembled by nanoparticles with size about 375-500 nm changed with reaction conditions. Room-temperature vibration magnetic strength measurements (VMS) demonstrates the as-obtained $ZnFe_2O_4$ submicrospheres show prefect superparamagnetism, whose coercivity force and remanence are practically nil. The reaction temperature and time influence on the crystallinity, diameter, saturated magnetic intensity and morphology of the particles.

Keywords: zinc ferrite; superparamagnetism; submicrospheres; nanoparticle; solvothermal

1. Introduction

Zinc ferrite as an important spinel oxide has been paid attention due to great potential in various technology applications (Sun *et al*. 2004). $ZnFe_2O_4$ as a desulfurization agent has the properties of the iron oxide's high temperature and zinc oxide's high precision desulfurization, it can recycling use. $ZnFe_2O_4$, as an antirust pigment, shows stable properties at the high temperature, such as non-toxic odorless, insoluble in acid and alkali and no migration in the plastic. $ZnFe_2O_4$ can be applied as the dehydrogenation catalyst of butene oxidative and visible light sensitive semiconductor. Many methods so far have been developed for synthesizing various zinc ferrite materials, such as electrospinning method (Han *et al*. 2014), lacto ferrin-assisted method (Wang *et al*. 2015), propylene oxide assisted sol-gel method (Bhosale *et al*. 2016), homogeneous precipitation method (Sharma and Ghose 2015), hydrothermal/solvothermal method (Surinwonga and Rujiwatrab 2013, Reddy and Mohamed 2015, Hu *et al*. 2011, George *et al*. 2006), and so on. Among of them, solvothermal method is an ideal approach for preparing $ZnFe_2O_4$ nanomaterials with excellent magnetism, crystal stability and special shapes. $ZnFe_2O_4$ submicrometer material

*Corresponding author, Associate Professor, E-mail: majie@usst.edu.cn
[a] Ms. Student, E-mail: 2811176608@qq.com
[b] Ms. Student, E-mail: 1427460876@qq.com
[c] Professor, E-mail: zhang_lucy9999@vip.126.com

 ISSN: 2287-237X (Print), 2287-2388 (Online)

will also show important application in many fields, such as magnetic separation, and catalysis. However, as we well known, it is rare report about how to prepare $ZnFe_2O_4$ submicrometer material with superparamagnetism.

In the present paper, we draw on the experience of a solvothermal route (Liu *et al*. 2009) and make some improvements for preparing MFe_2O_4 nanoparticles. It is firstly found that the one-pot solvothermal method can be successfully applied to obtain superparamagnetic $ZnFe_2O_4$ submicrospheres (López *et al*. 2012, Singh *et al*. 2015, Liu *et al*. 2000), the as-prepared $ZnFe_2O_4$ sample is self-assembled by nanoparticles and show well monodispersion and outstanding superparamagnetism. The solvothemal approach may be facile, environmentally and economically alternative method for preparing other kinds of MFe_2O_4-type ferrite submicromaterials.

2. Experimental

Ferric chloride ($6H_2O$), zinc chloride, anhydrous sodium acetate reaction in the ethylene glycol solvent synthesized zinc ferrite nanoparticles, All the reagents used in the experiment were at the highest purity and purchased from shanghai Chemical Reagent Lit.. In all experiment the deionized water derived from the water purification system (smart-s15) of lab.

2.1 Synthesized process

The one-pot solvothermal method is derived and improved from the literature (Liu *et al*. 2009), and some adjustments are made in the system. The typical procedure is described as follows: 0.0072 mol $FeCl_3$-$6H_2O$, 0.0036 mol $ZnCl_2$, 0.04 mol CH_3COONa (NaAc) and 70 mL glycol are put into three-necked flask. After the mixture is fully mixed about two hours, it is removed into 100 ml Teflon-lined stainless-steel autoclave. The autoclaves are sealed and settled in a digital-controlled constant temperature oven at 200- 215°C for 4-8 h. Then autoclaves are took out and cooled to room temperature naturally. As-obtained solid precipitation samples are washed with deionized water and absolute ethanol three times to make sure to remove excess electrolytes, organics. Finally, the product is obtained after it dried at 60°C for some hours.

2.2 Characterization

The crystal phase and purity of the product are characterized by X-ray powder diffraction (XRD, D8 advance). The power X-ray diffraction patterns were detected with a 2θ ranges from 20° to 80° at scanning rate 0.245 s/step. The morphologies of the ferrite magnetic nanomaterials were inspected by scanning electron microscopy (SEM, VEGA 3 SBH) at an accelerating voltage of 5.0 kV. The room-temperature magnetic property were detected by vibrating sample magnetometer (VSM, Lake Shore 735VSM, USA) in the range from -6000 to 6000 Oe.

3. Results and discussion

According to the typical SEM images of samples, we can find microspheres which composed of nanoparticles at the same reaction time with different reaction temperature. From Fig. 1(c) and Fig. 1(d), the size of samples is almost independent of reaction time, but the sample D is much

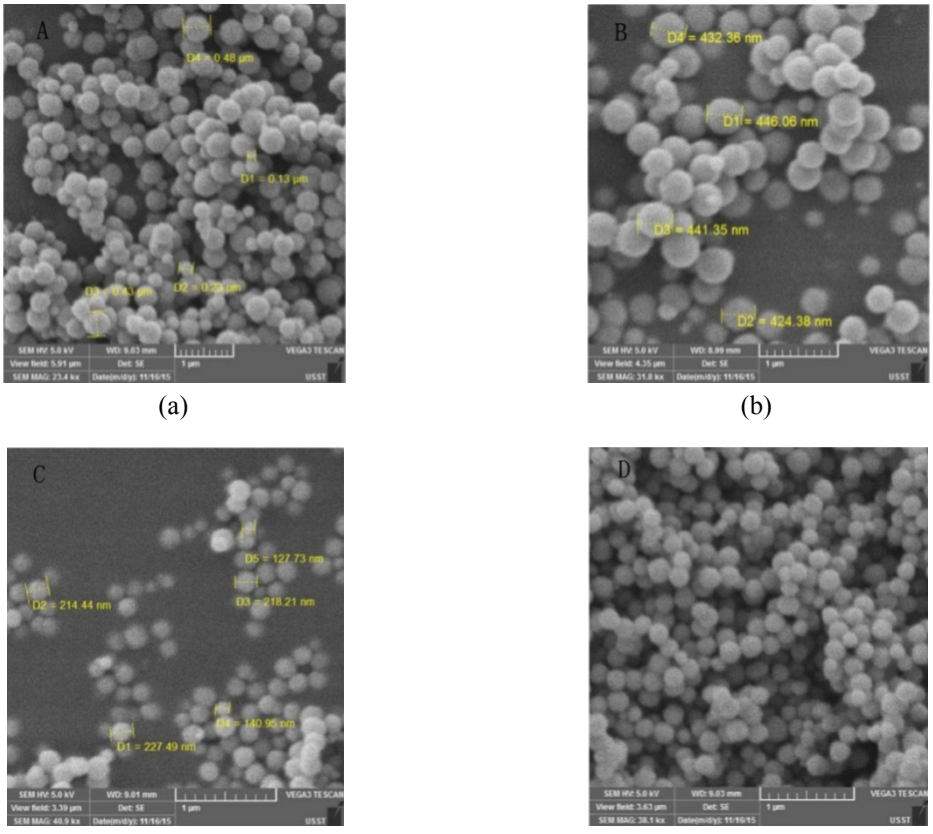

(a) (b)

(c) (d)

Fig. 1 SEM images of $ZnFe_2O_4$ obtained at 6 hours with different temperature: (a) 215°C; (b) 210°C; and (c) 200°C; respectively and (d) at 8 reaction time with 200°C

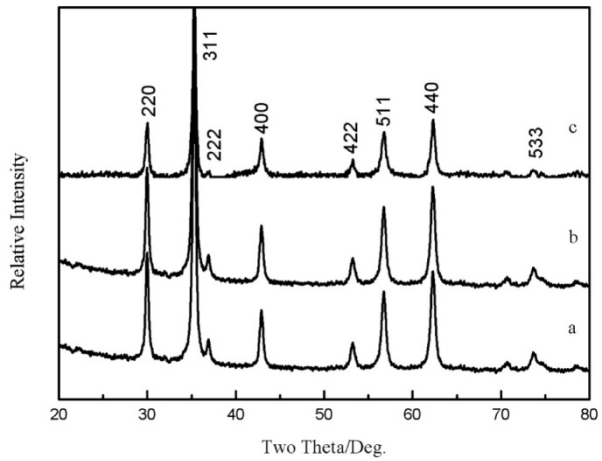

Fig. 2 The XRD patterns of $ZnFe_2O_4$ Powder obtained at reaction temperature of (a) 215°C; (b) 210°C; and (c) 200°C with the same reaction time at 8 hours

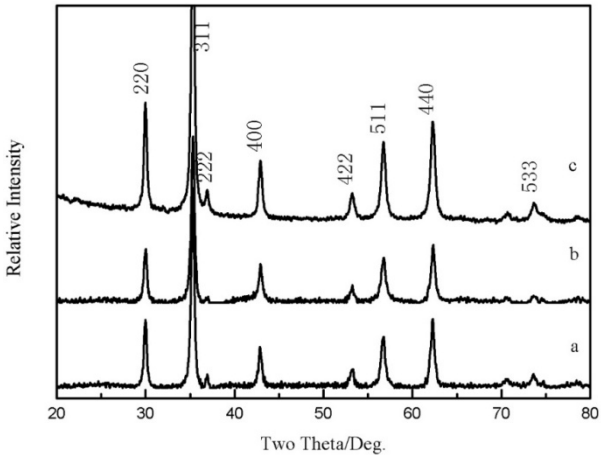

Fig. 3 The XRD patterns of $ZnFe_2O_4$ Powder obtained with the same temperature of 215°C at the different reaction time at (a) 8 hours; (b) 4 hours; and (c) 6 hours

better uniform then sample C. It indicates reaction time is benefit to improve monodispersion of as-obtained product.

The microspheres structure of $ZnFe_2O_4$ samples are characterized by XRD and relative results shown in Figs. 2 and 3. The diffraction peaks of all samples can easily be indexed as (2 2 0), (3 1 1), (2 2 2), (4 0 0), (4 2 2), (5 1 1), (4 4 0) and (5 3 3) planes of cubic structure and matches well with the standard data of $ZnFe_2O_4$ (JCPDS NO. 65-3111). The sizes of as-obtained samples, which are calculated by Scherrer equation, only slightly alter from 11.7 nm to 18.6 nm with change in reaction time. In the synthesis system, some glycol and its oligomer can be absorbed on the surface of nanoparticles and form an organic layer, which inhibits the growth of crystal size, so the size of sample does not increase obviously (Ma *et al*. 2013). Figs. 2(a) and 3(c) show the sharpest peak in all, which indicate the best crystalline product can be obtained at given conditions respectively.

The TEM images in Fig. 4 show the internal structure of different nanocubes samples. From the images we can easily find that C have the better dispersion and uniformity, with the increasing of reaction temperature, the ethylene glycol become more and more stick, between the ferrite like adding an isolation layer, each ferrite is separated and limited growth . The $ZnFe_2O_4$ nanoparticles in samples are spherical in shape, these submicrospheres are self-assembled by nanoparticles via a one-pot and the average nanoparticle sizes of $ZnFe_2O_4$ are from 375 nm to 500 nm. It is coincident with the above results detected with SEM and XRD.

The room-temperature magnetic properties of $ZnFe_2O_4$ nanoparticles obtained with the same reaction time at the different temperature are detected via VSM with an applied magnetic field of ±6000 Oe, Fig. 5 shows the room-temperature hysteresis loop of $ZnFe_2O_4$ submicrospheres and the corresponding evolution of magnetic parameters of saturation magnetization (Ms) and coercivity (Zhang *et al*. 2009, 2016, Kim *et al*. 2016, Luo *et al*. 2015, Nguyet *et al*. 2013, Kong *et al*. 2014) respectively. With the temperature rises, the saturation magnetic induction of the samples increased. Fig. 5(c) shows it has the maximum value of saturation magnetization beyond 100 emu/g, the above results indicate that the reaction temperature is benefit to improve the Ms value of product, which probably should be attributed to the crystallization of product promoted with the temperature increase.

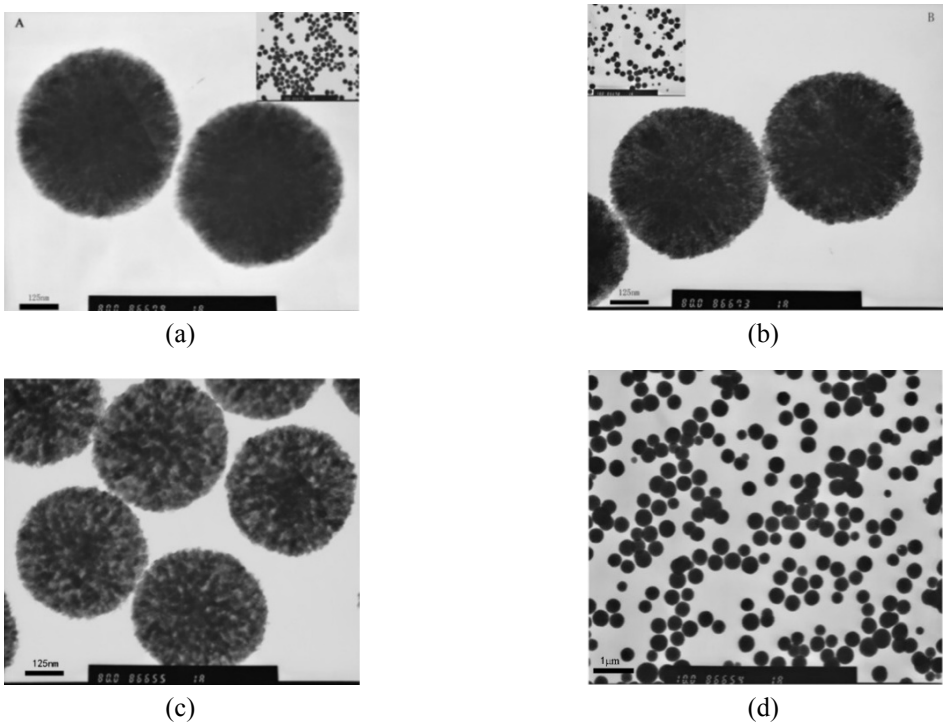

Fig. 4 The TEM images of $ZnFe_2O_4$ nanocubes obtained at (a) 200°C; (b) 210°C; and (c) & (d) 215°C for 6 hours

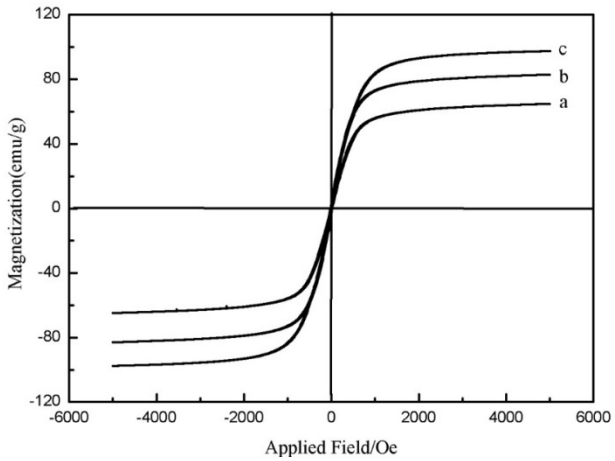

Fig. 5 The hysteresis loop of $ZnFe_2O_4$ nanoparticles obtained with the same reaction time (6h) at different reaction temperature (a) 200°C; (b) 210°C; and (c) 215°C

From the Fig. 6, by comparing the images of (a), (b) and (c), it is easily to find that the Fig. 6(c) has the lowest coercivity at the room-temperature, whose value can be negligible, this behavior reveals a characteristic of material with superparamagnetic properties. The images of Figs. 6(a)

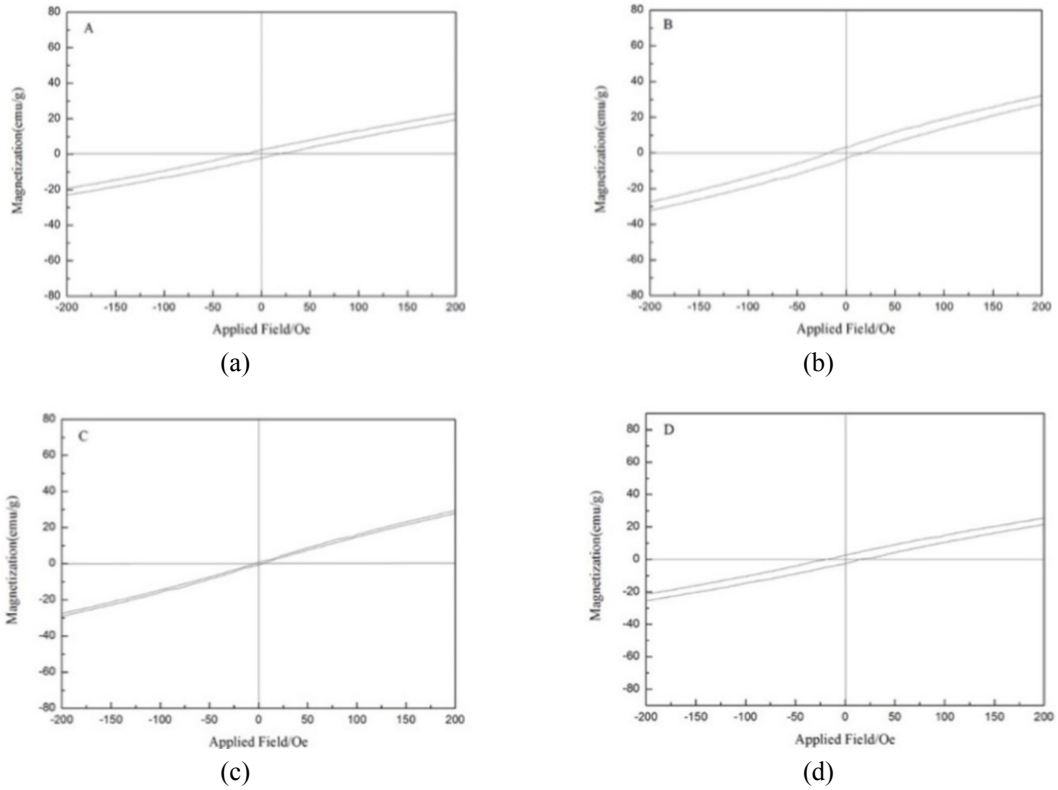

Fig. 6 The coercivity (Hc) field of $ZnFe_2O_4$ nanoparticles obtained with the same reaction time 6 hours at different temperature (a) 200°C; (b) 210°C; and (c) 215°C; respectively. (d) is at 200°C with 8 hours

and (d) demonstrate that at the room-temperature the coercivity (Hc) field with reaction time has no relationship (Silva *et al*. 2015). But the images of Figs. 6(b) and (c) show that with the increase of reaction temperature, the coercivity (Hc) field decreases, almost nearly zero. This result further confirms that it is very important to choose the appropriate reaction temperature for the preparation of superparamagnetic $ZnFe_2O_4$ material.

4. Conclusions

In summary, the $ZnFe_2O_4$ self-assembled submicrosphere are successfully synthesized via a modified one-pot solvothermal method. The method is performed at 215°C for 6 hours under template-free conditions. Zinc ferrite submicrosphers obtained at given conditions show excellent superparamagnetism with larger saturation magnetization and negligible coercivity and remanence. The average nanoparticle size of $ZnFe_2O_4$ is in range from 375 nm to 500 nm.

It will be further investigated if the one-pot solvothermal route can apply to prepare other ferrite self-assembled micrometer/nanometer materials, and further promote the application research about the superparamagnetic $ZnFe_2O_4$ submicrosphere in separation field, bio-medical field, and catalysis field, and so on.

Acknowledgments

The authors are thankful to the natural science foundation of Shanghai (No.15ZR1428500) and the national natural science foundation of China (No. 20906061) and for financial supports.

References

Bhosale, R.R., Kumar, A., Almomani, F. and Alxneit, I. (2016), "Sol-Gel derived CeO_2–Fe_2O_3 nanoparticles: Synthesis, characterization and solar thermochemical application", *Ceram. Int.*, **42**(6), 6728-6737.

George, M., John, A.M., Nair, S.S., Joy, P.A. and Anantharaman, M.R. (2006), "Finite size effects on the structural and magnetic properties of sol–gel synthesized $NiFe_2O_4$ powders", *J. Magn. Mater.*, **302**(1), 190-195.

Han, P., Jiang, X., Zhang, L., Yu, F., Shi, Q., Ding, Y. and Zhang, Q. (2014), "Effect of Li_2CO_3, flux on the preparation temperature, particle micro morphology and light absorption performance of samarium borate by solid state method", *J. Mater. Sci. Mater. Electron.*, **26**(2), 666-670.

Hu, P., Pan, D.A., Wang, X.F., Tian, J.J., Wang, J., Zhang, S.G. and Volinsky, A.A. (2011), "Fuel additives and heat treatment effects on nanocrystalline zinc ferrite phase composition", *Magn. Magn. Mater.*, **323**(5), 569-573.

Kim, S., Han, B.K., Quach, D.T., Kim, D.H., Kim, Y.K. and Choi-Yim, H. (2016), "Optimization of Fe/Co ratio in $Fe_{(87-x-y)}Co_xTi_7Zr_6B_y$ alloys for high saturation magnetization", *Curr. Appl. Phys.*, **16**(5), 515-519.

Kong, F.L., Chang, C.T., Inoue, A., Shalaan, E. and Al-Marzouki, F. (2014), "Fe-based amorphous soft magneticalloys with high saturation magnetization and good bending ductility", *J. Alloys Comp.*, **615**, 163-166.

Liu, C., Zou, B., Rondinone, A.J. and Zhang, Z.J. (2000), "Reverse micelle synthesis and characterization of superparamagnetic $MnFe_2O_4$ spinel ferrite nanocrystallites", *J. Phys. Chem. B*, **104**(6), 1141-1145.

Liu, S.H., Xing, R.M., Lu, F., Rana, R.K. and Zhu, J.J. (2009), "One-pot template-free fabrication of hollow magnetite nanospheres and their application as potential drug carriers", *J. Phys. Chem. C*, **113**(50), 21042-21047.

López, J., González-Bahamón, L.F., Prado, J., Caicedo, J.C., Zambrano, G., Gómez, M.E., Esteve, J. and Prieto, P. (2012), "Study of magnetic and structural properties of ferrofluids based on cobalt–zinc ferrite nanoparticles", *J. Magn. Mater.*, **324**(4), 394-402.

Luo, C., Fu, Y., Zhang, D., Yuan, S. and Zhai, Y. (2015), "Temperature dependent coercivity and magnetization of light rare-earth Nd doped permalloy thin films", *J. Magnet. Magnet. Mater.*, **374,** 711-715.

Ma, J., Zhao, J., Li, W.L., Zhang, S. and Tian, Z. (2013), "Preparation of cobalt ferrite nanoparticles via a novel solvothermal approach using divalent iron salt as precursors", *Mater. Res. Bull.*, **48**(2), 214-217.

Nguyet, D.T.T., Duong, N.P., Satoh, T., Anh, L.N. and Hien, T.D. (2013), "Magnetization and coercivity of nanocrystalline gadolinium iron garnet", *J. Magnet. Magnet. Mater.*, **332**, 180-185.

Reddy, M.P. and Mohamed, A.M.A. (2015), "One-pot solvothermal synthesis and performance of mesoporous magnetic ferrite MFe_2O_4 nanospheres", *Micropor. Mesopor. Mater.*, **215**, 37-45.

Sharma, R.K. and Ghose, R. (2015), "Synthesis of zinc oxide nanoparticles by homogeneous precipitation method and its application in antifungal activity against Candida albicans", *Ceram. Int.*, **41**(1), 967-975.

Silva, A.S., Franco, A., Pelegrini, F. and Dantas, N.O. (2015), "Paramagnetic behavior at room temperature of $Zn_{1-x}Mn_xTe$ nanocrystals grown in a phosphate glass matrix by the fusion method", *J. Alloys Compound.*, **647**, 637-643.

Singh, J.P., Gautam, S., Srivastava, R.C., Asokan, K. and Kanjilal, D. (2015), "Crystallite size induced crossover from paramagnetism to superparamagnetism in zinc ferrite nanoparticles", *Superlattices Microstruct.*, **86**, 390-394.

Sun, S.H., Zeng, H., Robinson, D.B., Raoux, S., Rice, P.M., Wang, S.X. and Li, G.X. (2004),

"Monodisperse MFe_2O_4 (M = Fe, Co, Mn) nanoparticles", *J. Am. Chem. Soc.*, **126**(1), 273-279.
Surinwonga, S. and Rujiwatrab, A. (2013), "Ultrasonic cavitation assisted solvothermal synthesis of superparamagnetic zinc ferrite nanoparticles", *Particuology*, **11**(5), 588-593.
Wang, X., Chen, L., Fan, Q., Fan, J. and Xu, G. (2015), "Lactoferrin-assisted synthesis of zinc ferrite nanocrystal: Its magnetic performance and photocatalytic activity", *J. Alloys Compound.*, **652**, 132-138.
Zhang, Q., Zhu, M., Zhang, Q., Li, Y. and Wang, H. (2009), "Fabrication and magnetic property analysis of monodisperse manganese–zinc ferrite nanospheres", *J. Magnet. Magnet. Mater.*, **321**(19), 3203-3206.
Zhang, Y., Li, X., Jing, J. and Zhao, Y. (2016), "Coercivity, microstructure and magnetization reversal mechanism in TiNi-doped L1FePt thin films", *J. Magnet. Magnet. Mater.*, **408**, 228-232.

JL